Available online at www.sciencedirect.com
ScienceDirect
Journal of Molecular Catalysis A: Chemical 273 (2007) 186–197
JOURNAL OF MOLECULAR CATALYSIS A: CHEMICAL
www.elsevier.com/locate/molcata

$Au/M_xO_y/TiO_2$ catalysts for CO oxidation: Promotional effect of main-group, transition, and rare-earth metal oxide additives

Zhen Ma, Steven H. Overbury, Sheng Dai *

Chemical Sciences Division, Oak Ridge National Laboratory, TN 37831, USA

Received 20 March 2007; received in revised form 2 April 2007; accepted 4 April 2007
Available online 8 April 2007

Abstract

Au/TiO_2 catalysts are active for CO oxidation, but they suffer from high-temperature sintering of the gold particles, and few attempts have been made to promote or stabilize Au/TiO_2. Our recent communication addressed these issues by loading gold onto Al_2O_3/TiO_2 prepared via surface-sol–gel processing of Al(*sec*-$OC_4H_9)_3$ on TiO_2 [W.F. Yan, S.M. Mahurin, Z.W. Pan, S.H. Overbury, S. Dai, J. Am. Chem. Soc. 127 (2005) 10480–10481]. In our current full paper, $Au/Al_2O_3/TiO_2$ catalysts were prepared alternatively by thermal decomposition of $Al(NO_3)_3$ on TiO_2 followed by loading gold, and the influences of the decomposition temperature and Al_2O_3 content were systematically surveyed. This facile method was subsequently extended to the preparation of a battery of metal oxide-modified Au/TiO_2 catalysts virtually not reported. It was found that Au/TiO_2 modified by CaO, NiO, ZnO, Ga_2O_3, Y_2O_3, ZrO_2, La_2O_3, Pr_2O_3, Nd_2O_3, Sm_2O_3, Eu_2O_3, Gd_2O_3, Dy_2O_3, Ho_2O_3, Er_2O_3, or Yb_2O_3 could retain significant activity at ambient temperature even after aging in O_2–He at 500 °C, whereas unmodified Au/TiO_2 lost its activity. Moreover, some 200 °C-calcined promoted catalysts showed high activity even at about −100 °C. The deactivation and regeneration of some of these new catalysts were studied. This work furnished novel catalysts for further fundamental and applied research.
Published by Elsevier B.V.

Keywords: Gold catalysis; CO oxidation; Titania; Metal oxide; Additive; Sintering

1. Introduction

Heterogeneous catalysis by gold, previously uncharted [1,2], has become an emerging field recently [3–5]. Supported gold catalysts have many applications in environmental control [6–9], chemical synthesis [10–13], energy generation [14,15], and materials processing [16,17]. In particular, Haruta et al. initially reported that supported gold nanoparticles were active for low-temperature CO oxidation [3,7]. However, due to the low melting point of gold nanoparticles, the sintering of gold catalysts above 400 °C is a drawback that may constrain their practical applications [7,18,19]. To address this issue, our group has used CO oxidation as a sensitive probe reaction [3–9], and studied different supports such as polymorphs of TiO_2 [20,21], Al_2O_3/TiO_2 [22], $Al_2O_3/TiO_2/SiO_2$ [23], PO_4^{3-}/TiO_2 [24], mesoporous [25] or fumed [26] SiO_2, and nano-crystalline $LaPO_4$ [27]. Particularly interesting is the finding that gold particles could be stabilized on Al_2O_3/TiO_2 synthesized via surface-sol–gel processing of Al(*sec*-$OC_4H_9)_3$ on TiO_2 [22,28]. Tai et al. [29] and Venezia et al. [30] reported parallel findings with TiO_2/SiO_2 supports prepared from Ti(*iso*-$OC_3H_7)_4$ precursor.

Although the performance of $Au/Al_2O_3/TiO_2$ is impressive [22,28], several questions remain unclear: (1) is the surface-sol–gel method necessary, or put it another way, is it possible to prepare $Au/Al_2O_3/TiO_2$ without involving non-aqueous condition, organic solvents, and aluminum alkoxide, while still achieving comparable performance? (2) Is "monolayer" [19,23] Al_2O_3 required, or what is the effect of the Al_2O_3 content? (3) Is Al_2O_3 unique, or will other metal oxide additives exhibit similar, or perhaps even better, promotional effect? (4) Are these modified gold catalysts stable on stream? As commented by Bond and Thompson, one of the unsatisfactory aspects of gold catalysis research is that possible changes in conversion with time on stream typically are not reported or only qualitatively mentioned [6]. In the literature, Au/Al_2O_3 is known to suffer from deactivation on stream [31,32], but the temporal stability of $Au/Al_2O_3/TiO_2$ has not been investigated [22,28].

* Corresponding author. Tel.: +1 865 576 7307; fax: +1 865 576 5235.
E-mail address: dais@ornl.gov (S. Dai).

1381-1169/$ – see front matter. Published by Elsevier B.V.
doi:10.1016/j.molcata.2007.04.007

The objective of the current work is not only to clarify these important issues, but also to explore novel gold catalysts promoted by metal oxides. In particular, we explored the promotion of Au/TiO_2 because few attempts have been made to promote it [3–9]. After demonstrating that $Au/Al_2O_3/TiO_2$ prepared via decomposition of $Al(NO_3)_3$ on TiO_2 could show comparable performance in CO oxidation as those made via surface-sol–gel processing of Al(*sec*-$OC_4H_9)_3$ [22], we extended this spontaneous dispersion method [33,34] to the preparation of a number of surface-modified TiO_2 supports. The key finding is that Au/TiO_2 modified by CaO, NiO, ZnO, Ga_2O_3, Y_2O_3, ZrO_2, La_2O_3, Pr_2O_3, Nd_2O_3, Sm_2O_3, Eu_2O_3, Gd_2O_3, Dy_2O_3, Ho_2O_3, Er_2O_3, or Yb_2O_3 could retain smaller gold particles and exhibit significant activity at ambient temperature even after aging at 500 °C, whereas unmodified Au/TiO_2 lost its activity. Moreover, some catalysts showed extraordinarily high activity as low as −100 °C. To the best of our knowledge, the promotion of Au/TiO_2 by these metal oxide additives for CO oxidation has virtually not been reported in the open literature. In our recent patent on surface-stabilized gold nanocatalysts [28], these freshly obtained findings were not claimed, either. Hence, this work furnished a novel gold catalyst system for further fundamental and applied research.

2. Experimental

$HAuCl_4·3H_2O$, TiO_2 (Degussa P25), $Al(NO_3)_3·9H_2O$, $Ca(NO_3)_2·4H_2O$, $Fe(NO_3)_3·9H_2O$ (EM), $Ni(NO_3)_2·6H_2O$, $Cu(NO_3)_2·2.5H_2O$, $Zn(NO_3)_2·6H_2O$, $Ga(NO_3)_3·xH_2O$, $Y(NO_3)_3·4H_2O$, $ZrO(NO_3)_2·xH_2O$, $(NH_4)_6Mo_7O_{24}·4H_2O$, $La(NO_3)_3·xH_2O$, $Ce(NO_3)_3·6H_2O$, $Pr(NO_3)_3·6H_2O$, $Nd(NO_3)_3·6H_2O$, $Sm(NO_3)_3·6H_2O$, $Eu(NO_3)_3·5H_2O$, $Gd(NO_3)_3·6H_2O$, $Dy(NO_3)_3·5H_2O$, $Ho(NO_3)_3·5H_2O$, $Er(NO_3)_3·5H_2O$, $Yb(NO_3)_3·5H_2O$, $(NH_4)_6H_2W_{12}O_{40}·xH_2O$, $H_3PW_{12}O_{40}·xH_2O$, $H_4SiW_{12}O_{40}·xH_2O$, and $Bi(NO_3)_3·5H_2O$ were obtained from Aldrich unless otherwise indicated.

Metal oxide-modified TiO_2 supports were prepared via excess-solution impregnation followed by spontaneous dispersion upon calcination [33,34]. A calculated amount of metal oxide precursor, usually a soluble metal nitrate, was dissolved in deionized water (typically 10 ml water per gram of TiO_2), and TiO_2 was subsequently added. The intended loading was 0.05 g M_xO_y per g TiO_2, except that for Al_2O_3/TiO_2, it was 0.01–1.0 g Al_2O_3 per gram of TiO_2. The slurry was magnetically stirred at room temperature until dry. The product was dried at 85 °C overnight, collected and ground into fine powders, and further calcined at 500 °C for 3 h (except that for the preparation of Al_2O_3/TiO_2, the $Al(NO_3)_3/TiO_2$ precursor was either not calcined or calcined at 200–700 °C). Al_2O_3 was prepared by calcining $Al(NO_3)_3·9H_2O$ at 500 °C for 3 h (except that in control experiments reported in Table S1 and Fig. S1 in the Supporting Information, it was not calcined or calcined at 100–800 °C).

Gold was loaded via a deposition–precipitation method [3–9]. First, 50 ml $HAuCl_4$ solution containing 0.3 g $HAuCl_4·3H_2O$ was poured into a beaker, and the pH value adjusted to 10.0 by 1.0 M KOH with vigorous stirring. The resulting solution was heated at 80 °C, 1.0 g support added, the beaker covered by a glass dish, and the slurry magnetically stirred for 2 h. The final pH value after deposition–precipitation was measured using a pH meter and recorded in Tables 2–4. The precipitate was centrifuged, washed three times with water and once with ethanol [20,22]. In each washing-centrifugation cycle, the solid deposited at the bottom of the centrifuge tube was re-dispersed using a vortexer, and then re-centrifuged. The final washing with ethanol [20,22] was found to reduce the supported gold precursor to metallic gold particles, analogous to the reduction of supported Ag^+ by formaldehyde [35] and that of Pd^{2+} by methanol [36]. The product was dried at 40 °C for 2 days, and referred to as "as-synthesized" catalyst. The catalyst was denoted as $Au/c\text{-}M_xO_y\text{-}d/TiO_2$, where c means the temperature used to calcine the M_xO_y/TiO_2 precursor and d the loading in terms of d g metal oxide per g TiO_2, and was simplified as $Au/M_xO_y/TiO_2$ if $c = 500$ and $d = 0.05$ (which is usually the case for the majority of catalysts reported here).

Catalytic CO oxidation was tested in a plug-flow microreactor (Altamira AMI 200). Typically, 50 mg catalyst was loaded into a U-shaped quartz tube (4 mm i.d.), except that in some stability tests, the catalyst load was less than 50 mg if the regular load (50 mg) would lead to 100% conversion. The exact catalyst load under such circumstances will be specified in Figs. 7–9. The catalyst was pretreated in flowing 5% O_2 (balance He) at 200 or 500 °C for 2.5 h. The catalyst was cooled down, the gas stream switched to 1% CO (balanced air) and the reaction temperature ramped using a furnace (at a rate of 0.5 °C/min above ambient temperature) or by immersing the U-shaped tube in ice-water or acetone–liquid nitrogen mixture to record the light-off curve. The flow rate of reactant stream was 37 cm^3/min, and the space velocity was 44,400 $cm^3/(h·g_{cat})$. A portion of the product stream was extracted periodically with an automatic sampling valve, and analyzed using a dual-column gas chromatograph with a thermal conductivity detector.

X-ray diffraction (XRD) data were collected on a Siemens D5005 diffractometer with Cu K_α radiation. Scans were performed at a rate of 0.01 °/s, typically in the range of $2\theta = 20$–85°. The average gold particle sizes were estimated from X-ray line broadening analysis applying the Debye–Scherrer equation on the (2 2 0) diffraction ($2\theta = 44°$) of gold. Elemental analysis was performed using inductivity coupled plasma-optical emission spectrometry (ICP-OES) on a Thermo IRIS Intrepid II spectrometer. Typically, accurately weighed 30–100 mg of sample was dissolved into HCl–HNO_3–HF acids at 70 °C, diluted by deionized water to 200 ml, and analyzed along with known solutions. BET surface areas of samples were measured by N_2 adsorption–desorption at 77 K using a Micromeritics Gemini instrument.

3. Results

3.1. $Au/Al_2O_3/TiO_2$ catalysts

3.1.1. General effects of Al_2O_3 surface modification

Fig. 1 depicts the light-off curves of Au/TiO_2, Au/Al_2O_3, and $Au/Al_2O_3/TiO_2$. The 200 °C-pretreated catalysts exhibited high activities, achieving T_{50} (temperature required for

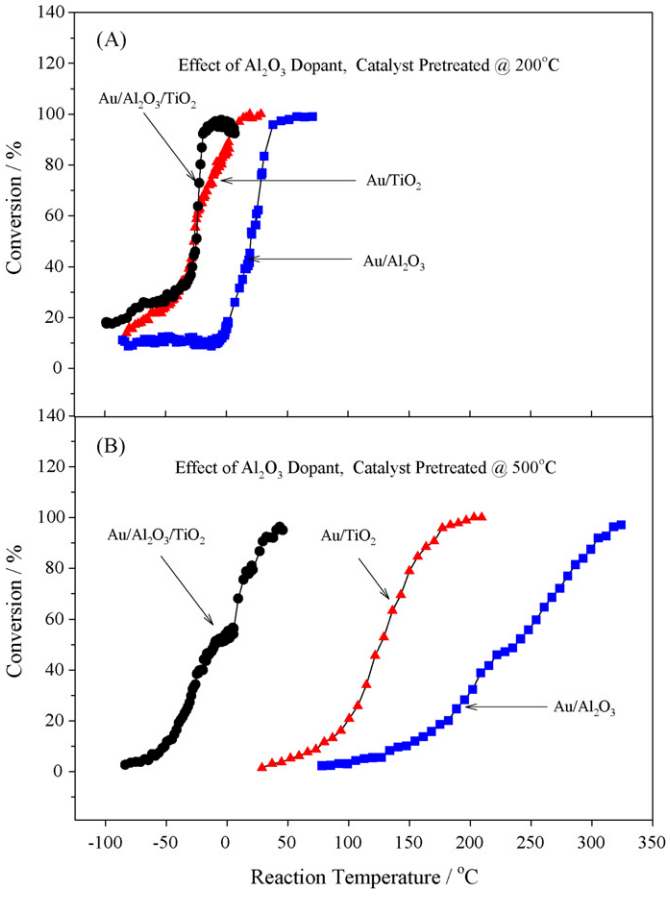

Fig. 1. CO light-off curves of Au/TiO_2 [24], Au/Al_2O_3, and $Au/Al_2O_3/TiO_2$ pretreated at 200 °C (A) or 500 °C (B).

50% conversion) values of −27, 20, and −25 °C, respectively (Fig. 1A). After 500 °C-aging, the T_{50} values of Au/TiO_2 and Au/Al_2O_3 increased dramatically to 126 °C [24] and 237 °C, respectively (Fig. 1B). The 126 °C value associated with 500 °C-aged Au/TiO_2 is consistent with the 125 °C value of 500 °C-aged Au/TiO_2 independently made and tested by Yan et al. [22]. Nevertheless, the T_{50} of 500 °C-aged $Au/Al_2O_3/TiO_2$ was maintained at −10 °C (Fig. 1B), comparable to the −17 °C value independently obtained by Yan in our group on $Au/Al_2O_3/TiO_2$ synthesized alternatively [22,28]. These data not only confirm the anti-aging effect previously observed by Yan et al. [22,28], but also suggest that the surface-sol–gel method is not necessary to get active $Au/Al_2O_3/TiO_2$.

Fig. 2 collects the XRD data of relevant supports and gold catalysts before and after reaction. In general, gold peaks appeared at $2\theta = 38°$, 44°, 65°, 78°, and 82°, corresponding to Au (1 1 1), (2 0 0), (2 2 0), (3 1 1), and (2 2 2), respectively [37]. In Fig. 2A, both TiO_2 (anatase and rutile) and gold were identified for Au/TiO_2 [24]. The gold peaks of the as-synthesized Au/TiO_2 were already obvious, due to the use of ethanol [20,22] to wash catalysts during the final stage of preparation (which is not absolutely necessary, but was consistently carried out in this work following the initial practice reported in Refs. [20,22]), analogous to the reduction of supported Ag^+ by formaldehyde [35] and that of Pd^{2+} by methanol [36]. In

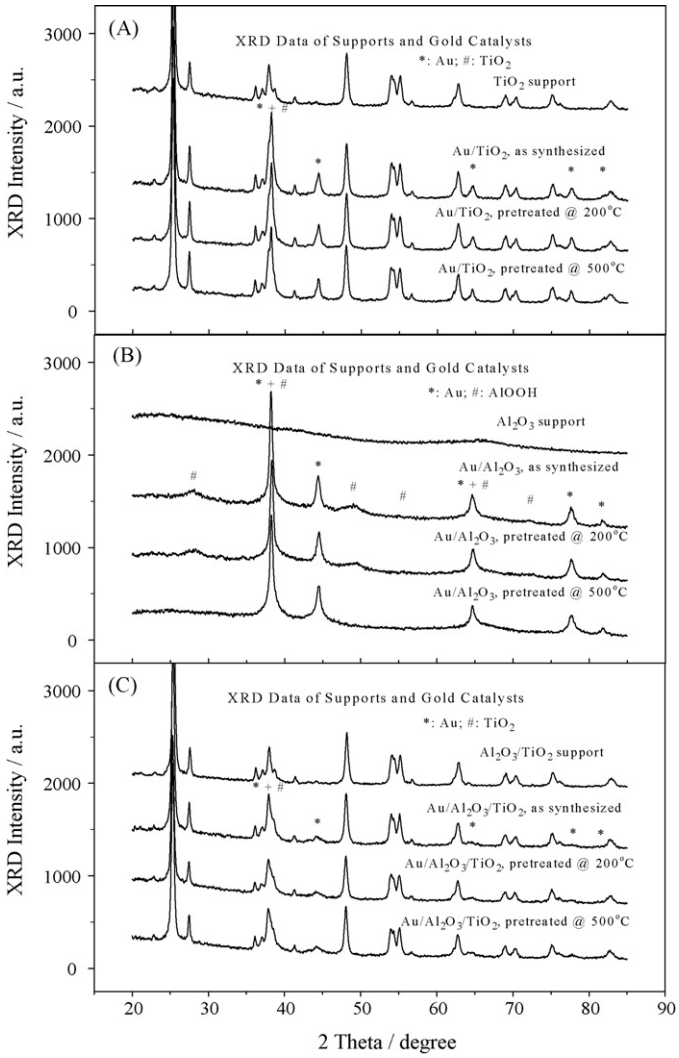

Fig. 2. XRD patterns of TiO_2, Al_2O_3, and Al_2O_3/TiO_2 supports, as well as as-synthesized Au/TiO_2 [24], Au/Al_2O_3, and $Au/Al_2O_3/TiO_2$ and those after 200 or 500 °C-pretreatments and light-off curve measurements.

Fig. 2B, Al_2O_3 derived from decomposition of $Al(NO_3)_3{\cdot}9H_2O$ at 500 °C showed broad features ascribed to amorphous Al_2O_3 [38]. In control experiments, nanocrystalline γ-Al_2O_3 was not formed until calcining $Al(NO_3)_3{\cdot}9H_2O$ at 800 °C (Fig. S1). After loading gold onto the amorphous Al_2O_3, what appeared were not only the expected gold peaks, but also new peaks at 28°, 49°, and 72°, indicating the formation of boehmite (AlOOH, also known as $Al_2O_3{\cdot}H_2O$) [39] after deposition–precipitation. The basic aqueous environment (pH ∼ 10) and the high solution temperature (80 °C) of deposition–precipitation may facilitate the formation of beohmite, as detected by XRD (Fig. 2B). The boehmite phase was maintained after 200 °C-treatment, but vanished after 500 °C-aging due to the release of crystal water [1], and the Al_2O_3 phase was again amorphous at that point. In Fig. 2C, only TiO_2 and gold phases could be clearly detected for $Au/Al_2O_3/TiO_2$.

After the structural and compositional analysis, the effect of Al_2O_3 surface modification on gold particle sizes was assessed. The Au (2 0 0) peaks ($2\theta = 44°$) of $Au/Al_2O_3/TiO_2$

Table 1
Surface areas and elemental analysis results of Al_2O_3/TiO_2 samples before and after loading gold

Entry	Support	Surface area (m^2/g)		Al content (wt%)	
		Before loading Au	After loading Au	Before loading Au	After loading Au
1	TiO_2	48.0	47.3	–	–
2	dry-Al_2O_3–0.05/TiO_2	26.9	47.7	1.89	1.96
3	200-Al_2O_3–0.05/TiO_2	32.9	40.5	1.98	1.94
4	300-Al_2O_3–0.05/TiO_2	40.1	40.5	2.11	2.11
5	400-Al_2O_3–0.05/TiO_2	42.4	42.4	2.21	2.16
6	500-Al_2O_3–0.05/TiO_2	42.2	42.2	2.21	2.18
7	600-Al_2O_3–0.05/TiO_2	43.5	43.9	2.21	2.16
8	700-Al_2O_3–0.05/TiO_2	43.4	44.0	2.23	2.16
9	500-Al_2O_3–0.01/TiO_2	47.0	44.2	0.24	0.21
10	500-Al_2O_3–0.04/TiO_2	46.8	50.0	1.94	1.78
11	500-Al_2O_3–0.2/TiO_2	38.3	102.0	8.60	8.39
12	500-Al_2O_3–0.5/TiO_2	64.6	186.7	17.1	16.2
13	500-Al_2O_3–1.0/TiO_2	86.4	172.0	23.9	20.1
14	500-Al_2O_3–from $Al(NO_3)_3$	18.3	112.9	45.5	37.7

(Fig. 2C) were much broader than those of Au/TiO_2 (Fig. 2A) and Au/Al_2O_3 (Fig. 2B), suggesting smaller gold particles for Au/Al_2O_3/TiO_2 [22]. Indeed, the average gold particle sizes of 500 °C-aged Au/TiO_2, Au/Al_2O_3, and Au/Al_2O_3/TiO_2 were estimated by XRD line-broadening method as 15.5, 10.9, and 6.9 nm, respectively. The average gold particle of 500 °C-aged Au/TiO_2 (15.5 nm), as estimated by X-ray line-broadening method, seems to be consistent with Yan et al.'s TEM study which showed gold particles generally larger than 5 nm, and up to 35 nm [22]. Although the X-ray line-broadening method can allow for the characterization of a sufficient amount of catalyst sample, gold particles smaller than 3 nm can hardly be detected because the peak is too broad, and the estimated average particle size is biased by the larger particles [40,41]. Nevertheless, our XRD data of 500 °C-aged catalysts may show the general trend, are in harmony with the trend seen in Ref. [22], and provide a possible explanation for the anti-aging effect observed in Fig. 1B.

3.1.2. *Effects of the calcination temperature of Al_2O_3/TiO_2*

Yan et al. loaded gold onto surface-sol–gel-derived Al_2O_3/TiO_2 that was dried but not calcined [22,28]. Herein, to study the influence of synthesis conditions, a first series of supports were prepared with or without calcining the $Al(NO_3)_3/TiO_2$ precursor. Their XRD patterns were identical to that of TiO_2 (Fig. S2).

Table 1 lists the measured surface areas and Al contents of various supports. The surface area of TiO_2 was 48.0 m^2/g. After impregnating of TiO_2 by $Al(NO_3)_3$ salt followed by drying at 85 °C, the surface area of the material decreased to 26.9 m^2/g, possibly due to the diluting effect of low-surface-area $Al(NO_3)_3$ (14.5 m^2/g after drying at 85 °C) and the plugging of

Table 2
Characterization results and catalysis data of Au/Al_2O_3/TiO_2 catalysts before and after reaction

Entry	Catalyst	Final pH	As synthesized		200 °C pretreated		500 °C pretreated	
			Au (wt%)	Au size (nm)	T_{50} (°C)	Au size (nm)	T_{50} (°C)	Au size (nm)
1	Au/TiO_2	9.1	5.6	11.6	−27	11.7	126	15.5, 16.2[a]
2	Au/dry-Al_2O_3–0.05/TiO_2	8.4	4.6	7.6	−31	7.5	−4	7.5
3	Au/200-Al_2O_3–0.05/TiO_2	8.5	5.8	7.3	−23	7.3	−4	7.3
4	Au/300-Al_2O_3–0.05/TiO_2	8.4	2.1	7.4	−33	7.4	9	7.4
5	Au/400-Al_2O_3–0.05/TiO_2	8.9	5.8	7.3	−21	7.5	11	7.4
6	Au/500-Al_2O_3–0.05/TiO_2	8.9	4.1	6.9	−25	7.0	−10	6.9, 6.9[a]
7	Au/600-Al_2O_3–0.05/TiO_2	9.2	3.9	6.8	−22	7.0	14	6.9
8	Au/700-Al_2O_3–0.05/TiO_2	9.0	3.2	6.4	−21	6.7	4	7.5
9	Au/500-Al_2O_3–0.01/TiO_2	9.0	3.4	8.6	−22	8.7	22	10.0
10	Au/500-Al_2O_3–0.04/TiO_2	8.9	3.2	8.3	−16	8.1	−8	8.7
11	Au/500-Al_2O_3–0.2/TiO_2	9.5	2.9	8.4	−3	8.5	−23	8.6
12	Au/500-Al_2O_3–0.5/TiO_2	9.4	3.7	9.1	79	9.1	−2	9.3
13	Au/500-Al_2O_3–1.0/TiO_2	9.2	5.1	9.3	61	9.1	11	9.7
14	Au/500-Al_2O_3–from $Al(NO_3)_3$	9.1	5.8	10.4	20	10.4	237	10.9

Final pH means the pH value of the aqueous phase after deposition–precipitation of gold, even though the initial pH value before deposition–precipitation was adjusted to 10.0. Gold contents were measured by ICP method. Average gold particle sizes were estimated using XRD line broadening method. The T_{50} (temperature-required for 50% conversion) values were read out from the corresponding light-off curves.

[a] Average gold particle sizes of the used catalysts collected after 120 h stability tests.

the pore structure of TiO_2 by the impregnated $Al(NO_3)_3$ salt. In a control experiment, $Al(NO_3)_3{\cdot}9H_2O$ and TiO_2 (0.368 g/1 g) were mechanically mixed and dried at 85 °C overnight. The surface area of the mixture was measured to be 42.0 m^2/g, consistent with the 42.2 m^2/g value calculated assuming solely the diluting effect, so the low surface area of $Al(NO_3)_3/TiO_2$ (26.9 m^2/g) should be due to both the diluting and plugging effects. Both the surface areas and Al contents of supports increased with the calcination temperature and leveled off at 400–700 °C (Table 1), indicating the more obvious decomposition of $Al(NO_3)_3$ below 400°C. The decomposition of $Al(NO_3){\cdot}9H_2O$ at elevated temperature to form Al_2O_3 is a well known process (Table S1 and Fig. S1) [38].

Table 1 also lists the surface areas and Al contents of as-synthesized catalysts. The surface area of uncalcined $Al(NO_3)_3/TiO_2$ was 26.9 m^2/g, but after loading gold, the surface area increased to 47.7 m^2/g (Table 1, entry 2). One possible explanation is that the impregnated $Al(NO_3)_3$ on TiO_2 got leached during deposition–precipitation, resulting in gold on bare TiO_2 (note that the surface area of bare TiO_2 was 48.0 m^2/g, close to the 47.7 m^2/g value mentioned above). However, the elemental analysis data indicated that the Al content was retained (Table 1, entry 2). Possibly, $Al(NO_3)_3/TiO_2$ was transformed to $Al(OH)_3/TiO_2$ in the basic media (pH ~ 10) of deposition–precipitation. Note that Al^{3+} is transformed to $Al(OH)_3$ at pH 9–10 [42].

Table 2 summarizes the catalytic performance. The T_{50} values of these 200 °C-pretreated $Au/Al_2O_3/TiO_2$ were in the range of −33 to −21 °C, and those of 500 °C-aged catalysts −10 to 14 °C, showing neither big differences nor clear-cut trends. As represented by the left trace in Fig. 1B, there were often dips or plateaus in the conversion curves, which certainly biased the precise determination of T_{50} values. These dips or plateaus were virtually not seen with $Au/PO_4^{3-}/TiO_2$ [24], but were seen with some of the catalysts reported here (Figs. 1, 3, 5 and 6) or elsewhere [25,43,44], explainable by the influence of carbonate [45–48]. In any case, under our experimental conditions, the catalytic performance of $Au/Al_2O_3/TiO_2$ is not significantly dependant on the calcination temperature of the modified support.

3.1.3. *Effects of Al_2O_3 content of Al_2O_3/TiO_2*

A second series of Al_2O_3/TiO_2 supports were prepared by tuning the Al_2O_3 content. When the Al_2O_3 content was increased from 0.01 to 1.0 g Al_2O_3 per g TiO_2, their XRD patterns were identical to that of TiO_2, except that the TiO_2 peaks were attenuated when the Al_2O_3 content was high (Fig. S2). The absence of Al_2O_3 peaks could be either due to the possibility that Al_2O_3 was not loaded, or due to the possibility that Al_2O_3 was amorphous. The elemental analysis results excluded the possibility that Al_2O_3 was not loaded (Table 1). This is expected, because according to the principle of impregnation, all of the Al in the $Al(NO_3)_3{\cdot}9H_2O$ precursor should be confined in the Al_2O_3/TiO_2 product. As for the second possibility, in fact, the Al_2O_3 derived from calcining $Al(NO_3)_3{\cdot}9H_2O$ at 500 °C was amorphous according to a XRD experiment (Fig. S1), and Yan et al. also did not observe any crystalline Al_2O_3 on $Au/Al_2O_3/TiO_2$ [22] or $Au/Al_2O_3/Al_2O_3/TiO_2$ [23]. Thus, Al_2O_3 could be highly dispersed on TiO_2 [33] or it might form a composite material with crystalline TiO_2 when the Al_2O_3 content was higher than the dispersion capacity of Al_2O_3 on TiO_2.

Table 1 compares the surface areas and Al contents of supports. The surface area of Al_2O_3 was 18.3 m^2/g, but that of Au/Al_2O_3 was 112.9 m^2/g. The bigger surface area of the latter is consistent with the formation of boehmite during deposition–precipitation preparation (Fig. 2B). Boehmite is known to exhibit bigger surface areas than amorphous Al_2O_3 [39]. Likewise, when the Al_2O_3 contents were larger than 0.2 g Al_2O_3 per g TiO_2, the surface areas of as-synthesized $Au/Al_2O_3/TiO_2$ were obviously bigger than those of corresponding Al_2O_3/TiO_2 supports (Table 1), possibly because the surface-area effect of boehmite became more apparent when the Al content was higher.

The catalytic data with respect to Al_2O_3 content was summarized in Table 2. The T_{50} values of these 200 °C-pretreated $Au/Al_2O_3/TiO_2$ catalysts (−25 to 79 °C) were comparable to that of 200 °C-pretreated Au/TiO_2 (−27 °C) only when the Al_2O_3 contents were low (0.01–0.05 g Al_2O_3 per g TiO_2), and increased to 70 or 61 °C when the Al_2O_3 content was 0.5 or 1.0 g Al_2O_3 per g TiO_2 (Table 2). The T_{50} values of these 500 °C-aged catalysts were in the range of −23 to 22 °C, and the effect of Al_2O_3 modification on stabilizing gold particles was apparent even when the Al_2O_3 content was 0.01 g Al_2O_3 per g TiO_2. Inter-

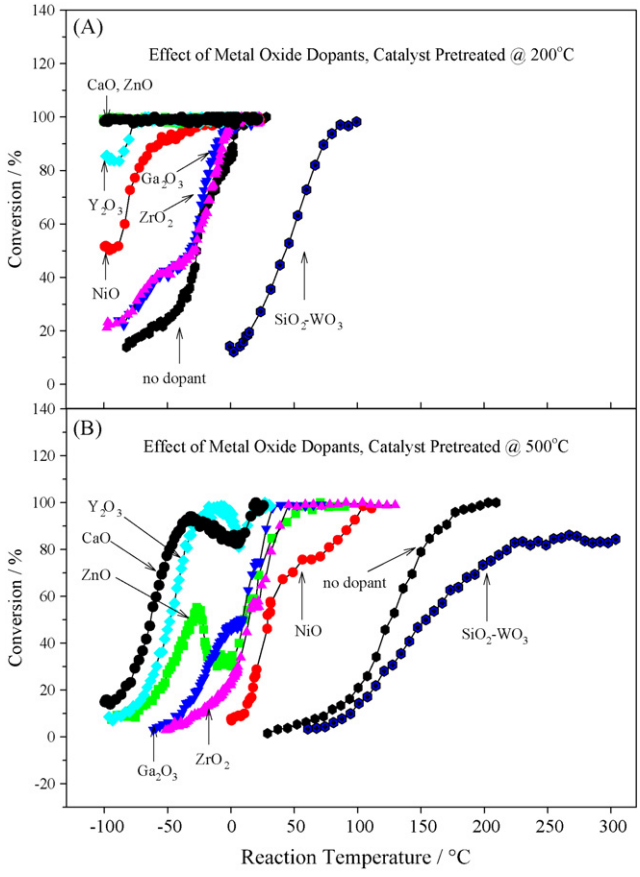

Fig. 3. CO light-off curves of unmodified [24] and CaO, NiO, ZnO, Ga_2O_3, Y_2O_3, ZrO_2, or SiO_2–WO_3 modified Au/TiO_2 catalysts pretreated at 200 °C (A) or 500 °C (B).

Table 3
Characterization results and catalysis data of $Au/M_xO_y/TiO_2$ catalysts before and after reaction

Entry	Catalyst	Final pH	Support	As synthesized			200 °C pretreated		500 °C pretreated	
			BET (m^2/g)	BET (m^2/g)	Au (wt%)	Au size (nm)	T_{50} (°C)	Au size (nm)	T_{50} (°C)	Au size (nm)
1	Au/TiO_2	9.1	48.0	47.3	5.6	11.6	−27	11.7	126	15.5 (16.2[a])
2	$Au/CaO/TiO_2$	9.1	34.8	37.3	11.4	6.0	<−100	6.0	−63	6.2
3	$Au/Fe_2O_3/TiO_2$	9.5	44.4	41.3	3.7	5.6	−26	6.0	25	6.2
4	$Au/NiO/TiO_2$	9.0	41.7	41.6	4.3	6.9	<−100	7.3	29	8.1
5	$Au/CuO/TiO_2$	10.2	39.4	37.1	2.6	4.9	4	5.2	31	6.4
6	$Au/ZnO/TiO_2$	10.0	38.8	41.3	3.0	5.7	<−100	5.6	−31	6.5 (6.9[a])
7	$Au/Ga_2O_3/TiO_2$	8.4	47.1	44.6	3.7	9.1	−32	9.0	9	9.3 (9.3[a])
8	$Au/Y_2O_3/TiO_2$	9.1	46.4	43.6	5.7	5.2	<−100	5.4	−48	6.4 (6.2[a])
9	$Au/ZrO_2/TiO_2$	9.6	48.2	42.6	2.7	5.6	−30	5.6	14	6.3 (6.2[a])
10	$Au/MoO_3/TiO_2$	7.2	53.0	45.4	8.3	10.5	25	10.9	202	16.9
11	$Au/WO_3/TiO_2$	8.9	50.3	51.8	2.0	9.1	31	9.1	124	9.2
12	$Au/SiO_2–WO_3/TiO_2$	7.9	48.2	45.5	3.9	9.2	43	9.2	154	11.0
13	$Au/P_2O_5–WO_3/TiO_2$	8.5	50.5	47.1	2.8	8.4	34	8.9	146	10.1
14	$Au/Bi_2O_3/TiO_2$	9.5	47.2	42.8	5.2	8.1	−31	8.1	156	9.5

[a] Average gold particle sizes of the used catalysts collected after 120 h stability tests.

estingly, some 500 °C-aged $Au/Al_2O_3/TiO_2$ catalysts were even more active than the corresponding 200 °C-aged ones when the Al_2O_3 contents were in the range of 0.2–1.0 g Al_2O_3/TiO_2. This thermal activation is quite surprising but resembles our previous finding that 500 °C-aged $Au/LaPO_4$ and Au/TiO_2/AlOOH could be more active than the as-synthesized ones [27,28].

3.2. Extension to other metal oxide additives

The key idea of modifying TiO_2 with Al_2O_3 for supporting gold was extended to a number of main group, transition, and rare earth metal oxide additives. The XRD patterns of these modified supports were identical to that of TiO_2 (Figs. S3 and S4), and their surface areas, in most cases, were close to that of TiO_2 (Tables 3 and 4).

3.2.1. Effects of main-group and transition metal oxide additives

Fig. 3A shows the light-off curves of 200 °C-pretreated $Au/M_xO_y/TiO_2$ (M = Ca, Ni, Zn, Ga, Y, Zr, and Si–W). Among these additives, Ga_2O_3 and ZrO_2 virtually did not change the activity, CaO, NiO, ZnO, and Y_2O_3 significantly promoted Au/TiO_2, and $SiO_2–WO_3$ reduced the activity. In particular, $Au/CaO/TiO_2$, $Au/NiO/TiO_2$, $Au/ZnO/TiO_2$, and $Au/Y_2O_3/TiO_2$ exhibited anomalously high activity about −100 °C, even though these catalysts were sufficiently cooled at −100 °C. In the literature, virtually no supported gold catalysts could be so active at −100 °C [3–9]. Even for the highly active $Au/LaPO_4$, its activity was less than 20% about −100 °C [27,28]. Nevertheless, the similar anomalous activity was observed in our previous investigation of CO oxidation on H_2-reduced $Au/TiO_2/TiO_2/SiO_2$ and $Au/Al_2O_3/TiO_2/SiO_2$, but no high activity was found after calcination of these catalysts in O_2–He [23]. It should be mentioned that the high activity at −100 °C may not be due to the stoichiometric reaction between Au^{3+} and CO: after measuring the light-off curve of 200 °C-pretreated $Au/Y_2O_3/TiO_2$, we cooled down the catalyst to −100 °C, and found that the high activity was still there (data not shown).

Table 4
Characterization results and catalysis data of $Au/RE_xO_y/TiO_2$ catalysts before and after reaction

Entry	Catalyst	Final pH	Support	As synthesized			200 °C pretreated		500 °C pretreated	
			BET (m^2/g)	BET (m^2/g)	Au (wt%)	Au size (nm)	T_{50} (°C)	Au size (nm)	T_{50} (°C)	Au size (nm)
1	Au/TiO_2	9.1	48.0	47.3	5.6	11.6	−27	11.7	126	15.5 (16.2[a])
2	$Au/La_2O_3/TiO_2$	10.4	43.7	42.5	3.5	5.6	−75	5.6	−39	6.1 (6.1[a])
3	$Au/CeO_2/TiO_2$	9.4	45.5	44.3	3.6	9.0	−19	9.1	49	9.2
4	$Au/Pr_2O_3/TiO_2$	9.8	45.4	43.4	5.2	6.7	<−100	6.7	16	6.6
5	$Au/Nd_2O_3/TiO_2$	9.6	44.0	42.3	4.8	7.6	<−100	7.4	−42	7.9
6	$Au/Sm_2O_3/TiO_2$	9.7	45.8	44.2	4.0	6.7	<−100	6.9	−31	7.3
7	$Au/Eu_2O_3/TiO_2$	9.8	44.7	47.6	4.4	6.3	<−100	6.1	−46	6.3
8	$Au/Gd_2O_3/TiO_2$	9.7	45.0	43.0	3.9	6.7	−78	6.9	−12	7.1
9	$Au/Dy_2O_3/TiO_2$	9.7	44.6	43.5	4.2	6.6	−88	6.8	−17	7.0
10	$Au/Ho_2O_3/TiO_2$	9.1	45.0	45.8	2.6	7.3	<−100	7.2	−25	8.0
11	$Au/Er_2O_3/TiO_2$	9.4	45.8	44.6	4.8	6.1	<−100	6.1	−33	7.0
12	$Au/Yb_2O_3/TiO_2$	9.6	46.3	42.1	4.3	7.0	<−100	7.0	−29	7.3

[a] Average gold particle sizes of the used catalysts collected after 120 h stability tests.

Fig. 3B shows the light-off curves of 500 °C-pretreated $Au/M_xO_y/TiO_2$ (M = Ca, Ni, Zn, Ga, Y, Zr, and Si–W). The T_{50} values of 500 °C-aged Au/TiO_2 and $Au/SiO_2–WO_3/TiO_2$ increased dramatically to 126 and 154 °C, respectively, whereas those of $Au/CaO/TiO_2$, $Au/NiO/TiO_2$, $Au/ZnO/TiO_2$, $Au/Ga_2O_3/TiO_2$, $Au/Y_2O_3/TiO_2$, and $Au/ZrO_2/TiO_2$ were −63, 29, −31, 9, −48, and 14 °C, respectively. In particular, 500 °C-aged $Au/CaO/TiO_2$, $Au/Y_2O_3/TiO_2$, and $Au/ZnO/TiO_2$ (Fig. 3B) exhibited even higher activities than 500 °C-aged $Au/Al_2O_3/TiO_2$ (Fig. 1B) at low temperature. These T_{50} values were even lower than the −17 °C value of $Au/Al_2O_3/TiO_2$ synthesized using the surface-sol–gel method [22,28]. There were again dips in their light-off curves, implying the influence of carbonate [45–48].

The drastic difference in T_{50} value can certainly show the activity trend, but because the gold loadings of catalysts are different (Table 2), specific rates were calculated (Table S2). To compare the activity using specific rates of different catalysts, it is important to make sure that the specific reaction temperature chosen is not so high that the conversions all reach 100%. Thus, the CO conversion at −80 °C for 200 °C-pretreated gold catalysts and that at −25 °C for 500 °C-aged catalysts were used for calculating specific rates. The majority of the catalysts reported here have activity at these temperatures under the respective pretreatment conditions. As shown in Table S2, the promotional effects of the beneficial metal oxide additives reported above are still apparent.

Fig. 4 summarizes the XRD patterns of $Au/M_xO_y/TiO_2$ (M = Ca, Ni, Zn, Ga, Y, Zr, and Si–W) after 500 °C-aging and light-off curve measurements. The 500 °C-aged Au/TiO_2 exhibited relatively sharp gold peaks, corresponding to big gold particles and poor activity. However, the gold peaks of 500 °C-aged $Au/CaO/TiO_2$, $Au/NiO/TiO_2$, $Au/ZnO/TiO_2$, $Au/Ga_2O_3/TiO_2$, $Au/Y_2O_3/TiO_2$, and $Au/ZrO_2/TiO_2$ were much broader, indicating the stabilizing of gold particles by these metal oxide additives. This is similar to the effect of Al_2O_3 additive [22] (Fig. 2C), and consistent with the high activities in Fig. 3B. On the other hand, the gold peaks of 500 °C-aged $Au/SiO_2–WO_3/TiO_2$ were sharp, consistent with its low activity. Nevertheless, it should be kept in mind that gold particle size is only one of the factors that may influence the catalytic performance [3–9]. In fact, from Table 2, it is observed that catalysts with similar average gold particle sizes could have different activity. This should be attributed to the influence of factors other than gold sizes (e.g., the nature of the support is different when using this additive compared to another [3,43,49,50]) as well as the limitation of XRD methods [40,41].

3.2.2. *Effects of rare-earth metal oxide additives*

Although some neat rare earth metal oxides have been used to support gold [51–53], to the best of our knowledge, the promotion of Au/TiO_2 by rare earth metal oxides for CO oxidation was virtually not reported. Figs. 5 and 6 show that, many rare earth metal oxides could promote Au/TiO_2 for CO oxidation. They, except for CeO_2, again exhibited anomalous activity at −100 °C when they were pretreated at 200 °C, and they were very active below 0 °C even after aging at 500 °C. The specific rates were calculated, and the promotional effect of the beneficial metal oxide additives mentioned above is obvious (Table S3). The average gold particle sizes of these catalysts, estimated by XRD experiments, were all smaller than those of Au/TiO_2 (Table 4).

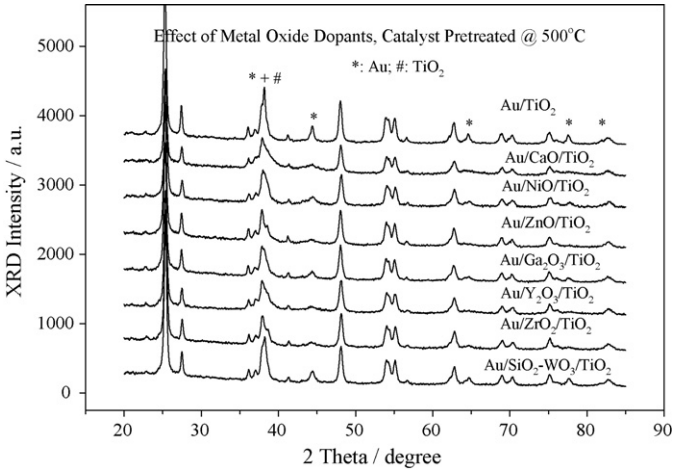

Fig. 4. XRD patterns of unmodified [24] and CaO, NiO, ZnO, Ga_2O_3, Y_2O_3, ZrO_2, or $SiO_2–WO_3$ modified Au/TiO_2 catalysts after 500 °C-treatments and light-off curve measurements.

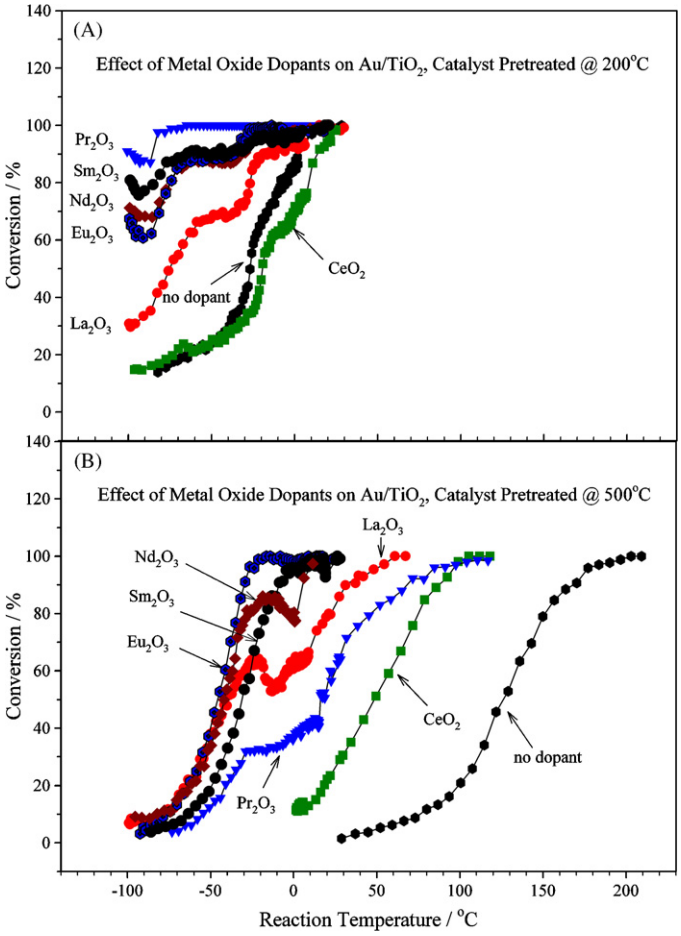

Fig. 5. CO light-off curves of unmodified [24] and La_2O_3, CeO_2, Pr_2O_3, Nd_2O_3, Sm_2O_3, or Eu_2O_3-modified Au/TiO_2 catalysts pretreated at 200 °C (A) or 500 °C (B).

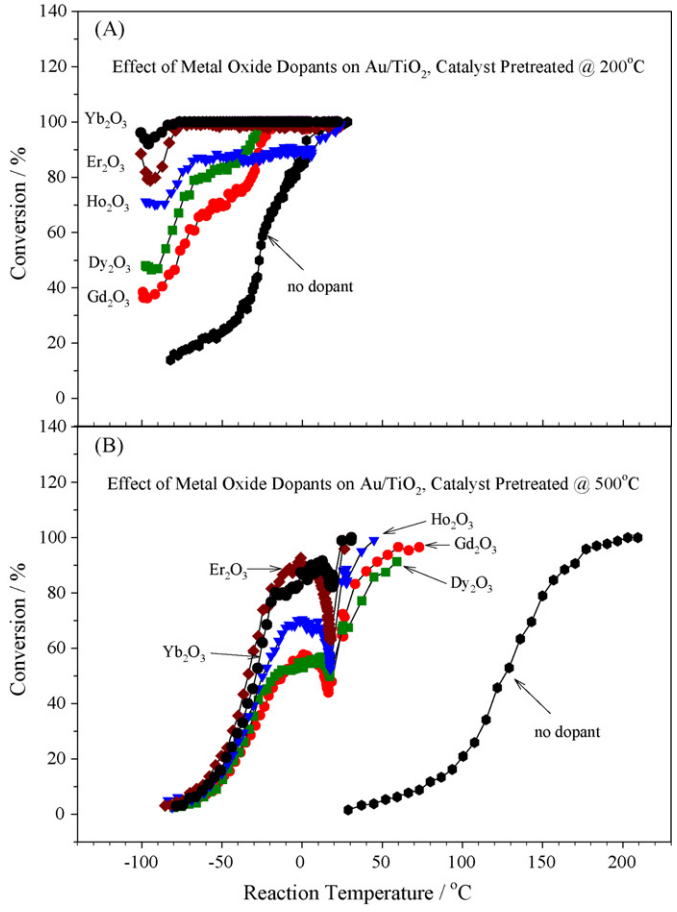

Fig. 6. CO light-off curves of unmodified [24] and Gd_2O_3, Dy_2O_3, Ho_2O_3, Er_2O_3, or Yb_2O_3–modified Au/TiO_2 catalysts pretreated at 200 °C (A) or 500 °C (B).

However, it should be mentioned again that gold particle size is not the only factor that determines activity [3–9].

3.3. Stability tests as a function of reaction time and regeneration

Stability means the ability of the catalyst to maintain a constant level of performance during the course of reaction [2]. Some research did not report stability [20,22,23,27,54], or mentioned vaguely that no deactivation was detected [55,56]. Sometimes, the catalyst load or reaction temperature was higher than just needed for complete conversion, resulting in 100% conversion for a long time [57–59]. However, others cautioned that in order to clarify the stability trends, it is crucial to make sure that the conversion would not reach 100% [5,60]. Indeed, our control experiments indicated that a misleading picture of stability could be obtained if the catalyst load or reaction temperature exceeded more than needed (Fig. 7), although such practice may be useful for practical purposes to compensate the loss in activity [61].

Specifically, in Fig. 7, when 50 mg $Au/ZnO/TiO_2$ was loaded, the steady-state conversion was about 30%. When 100 mg catalyst was loaded and the flow rate of the reactant stream was the same (37 cm^3/min), the steady-state conversion increased

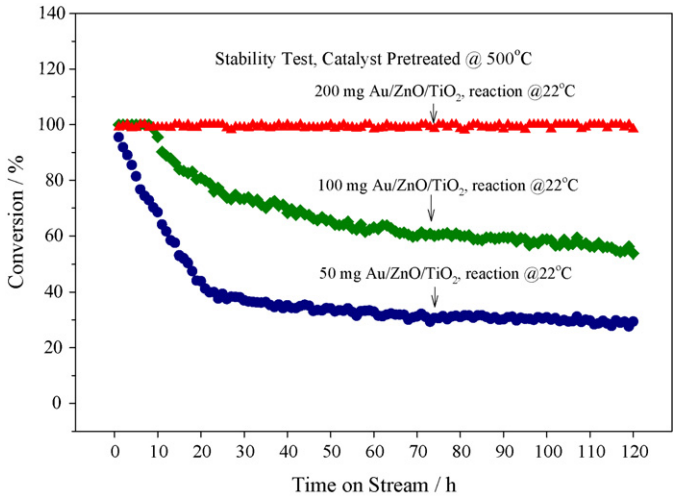

Fig. 7. Effects of the load of $Au/ZnO/TiO_2$ catalyst in the reactor on the CO conversion with time on stream. The catalyst was aged at 500 °C, and tested for 120 h. The flow rate of reactant stream was 37 cm^3/min.

to about 60%. This is expected, assuming that the number of active sites is doubled when doubling the amount of catalyst loaded in the reactor [5]. Thus, conceptually, the steady-state conversion should increase with the catalyst load until reaching 100%. Indeed, we found that the conversion was always close to 100% if we put 200 mg catalyst in the reactor (Fig. 7). However, the fact that no deactivation was observed (always 100% conversion) should not be used as grounds to claim that a catalyst has high stability on stream. This pitfall, sometimes overlooked, was critically discussed in recent reviews [5,61].

With these considerations, we properly tested the stability of typical 500 °C-calcined $Au/M_xO_y/TiO_2$ catalysts, loading less catalyst if the regular load (50 mg) would lead to 100% conversion at room temperature [5], and testing the stability for sufficient duration of time if several hours are deemed insufficient [34,60,62]. As shown in Fig. 8, the CO conversion of 500 °C-aged Au/TiO_2 at 170 °C dropped from ca. 93 to 89% during 5 days [24], consistent with the trend seen in the literature [50,62,63]. However, the temporal stability of $Au/M_xO_y/TiO_2$ catalysts was poorer. They often underwent initial faster deactivation, and the conversions leveled off later, implying the formation of less reactive intermediates on catalyst surfaces [45–48]. In particular, the activity of $Au/Al_2O_3/TiO_2$ was decreasing on stream, consistent with others' finding that Au/Al_2O_3 suffered from deactivation on stream because of the influence of carbonate [31,32]. For comparison purposes, the catalytic stability of our $Au/Al_2O_3/TiO_2$ catalysts previously synthesized via the surface-sol–gel method [22,28] was investigated. These catalysts also suffered from some deactivation on stream (Fig. S5) [22,28]. The deactivation of $Au/ZnO/TiO_2$ seems to contradict the observation by Zhang et al., who claimed that the conversion of CO on a large quantity of Au/ZnO could be maintained at 100% for months followed by observable deactivation [57]. Nevertheless, our data are in line with their another observation that some less active Au/ZnO with initial CO conversions lower than 100% deactivated quickly [58], and with the finding by Scurrell et al. that $Au/ZnO/TiO_2$ deactivated more

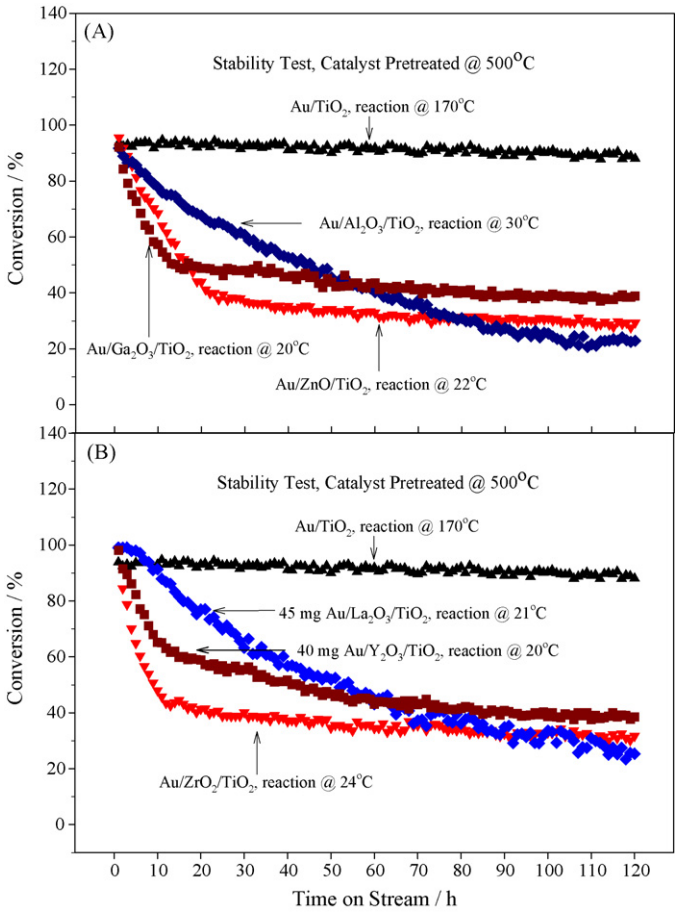

Fig. 8. CO conversion as a function of time on stream. The catalysts were aged at 500 °C, and tested for 120 h. Unless otherwise indicated, 50 mg catalyst was loaded, and the flow rate of reactant stream was 37 cm^3/min. The stability data of 500 °C-aged Au/TiO_2 [24] was plotted for comparison.

quickly than Au/TiO_2 [64]. Others have found deactivation in Au/ZrO_2 [45,48], whereas the deactivation of Au/TiO_2 was often less obvious [50,63,65]. These exist some references mentioning that the deactivation of some gold catalysts are due to the accumulation of carbonate, although the growth of gold particles under high-reaction-temperature conditions is also possible [3,45–48]. Nevertheless, we noted that under our low-reaction-temperature conditions, the growth of gold particles was not obvious (Tables 2, 3 and 4).

Given the fact of deactivation on stream, the next step is to regenerate the catalyst after deactivation and to develop methods for suppressing the temporal deactivation. Concerning the first idea, we carried out a preliminary regeneration experiment, in which 100 mg 500 °C-aged $Au/ZnO/TiO_2$ catalyst, subject to the 120 h stability test in Fig. 7 and stored in the U-type tube afterwards at ambient temperature for weeks, was treated in O_2–He at 400 °C for 1 h, and cooled down to ambient temperature for reaction. The initial activity of the regenerated catalyst at ambient temperature returned to 100%, indicating that the activity of the deactivated catalyst could at least be partially restored. In fact, we recently studied the regeneration of Au/Al_2O_3 and $Au/TiO_2/Al_2O_3$ catalysts initially reported in our patent [28], as well as the regeneration of other catalysts not reported yet,

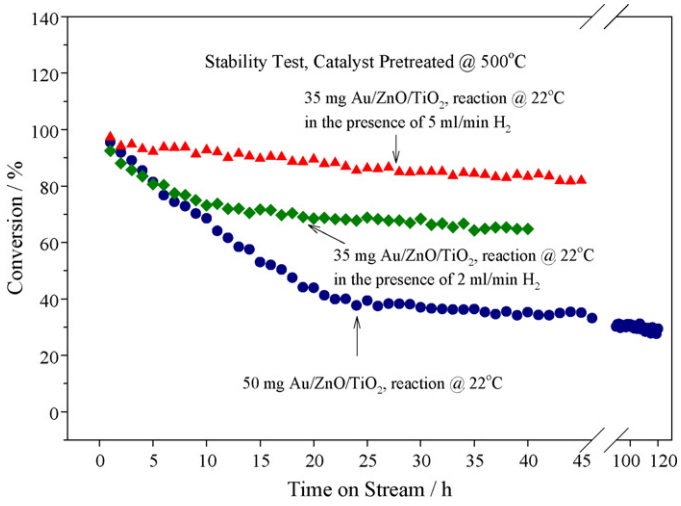

Fig. 9. The deactivation of $Au/ZnO/TiO_2$ in the absence or presence of H_2. The catalysts were aged at 500 °C before testing. In one run, 50 mg catalyst was loaded, and no H_2 was added. In other two runs, 35 mg catalyst was loaded, and the H_2 flow rate was 2 or 5 ml/min, with the 1% CO rate 37 ml/min.

and found that many of these catalysts could be regenerated that way, by treating the used catalysts in O_2–He at 400 °C (data not shown). The regeneration of gold catalysts is a topic worth further research [9,66].

Concerning the suppressing of deactivation, Yan et al. in our group have recently found that the deactivation of $Au/AlPO_4$ on stream could be eliminated in the presence of H_2, arguably via suppressing the build-up of carbonate [28]. In fact, this interesting phenomenon has already been noticed by others [67,68]. In the current study, we found that the deactivation of $Au/ZnO/TiO_2$ was suppressed to some extent (Fig. 9), if 2 ml/min pure H_2 was co-fed with the regular reactant stream (1% CO, 37 ml/min). During the tested period, around 30% of the H_2 gas was consumed. In another run, 5 ml/min H_2 was added, and the deactivation was further suppressed (Fig. 9). During that period, around 20% of the H_2 gas was consumed. It was proposed in the literature that the formation of water from H_2 oxidation may clean up the surface carbonate species, thus suppressing the deactivation of gold catalysts [9,67,68]. Further spectroscopic experiments could be very worthwhile.

4. Discussion

Gold catalysis is a hot topic, with tens of papers published weekly [4]. However, most of the gold catalysts were synthesized by loading gold onto neat, but not surface-modified, metal oxides [3–9]. This situation is in contrast to the research on mesoporous materials [69], solid strong acids [70], and semiconductor photocatalysts [71], in which the use of metal oxide promoters has become very popular.

To address such imbalance, our group recently communicated that Al_2O_3 additive on TiO_2 could stabilize gold particles and suppress the thermal aging [22], but it was not clear from that communication whether the use of an additive such as Al_2O_3 [22] to stabilize gold particles is a serendipitous choice, or represents a general methodology. The key contribution of our current

work is not only to confirm the effects of Al_2O_3, but also to demonstrate for the first time that an array of other additives, such as CaO, NiO, ZnO, Ga_2O_3, Y_2O_3, ZrO_2, La_2O_3, Pr_2O_3, Nd_2O_3, Sm_2O_3, Eu_2O_3, Gd_2O_3, Dy_2O_3, Ho_2O_3, Er_2O_3, and Yb_2O_3 on TiO_2 could exhibit similar or even better effects. The key advantages of the synthesis method used here [33,34], compared to the surface-sol–gel method [22,28], are that it adopts simple steps, avoids non-aqueous environments, uses water instead of organic solvents, and avoids the use of expensive metal alkoxides.

To place our work in proper perspective, the use of modified metal oxides on gold catalysis is summarized. Since Au/SiO_2 and Au/Al_2O_3 are inherently less active than Au/TiO_2 for CO oxidation, some attempts have been made to modify the underlying SiO_2 and Al_2O_3 supports in order to make them more active. For instance, SiO_2 was modified by Al_2O_3 [23,72], TiO_2 [29,30,54,73–75], Fe_2O_3 [62], CoO_x [41,72,76,77], LaO_x [76], and CeO_x [76], and then loaded with gold for CO oxidation [23,29,30,41,54,62,72,76,77] and propylene epoxidation [73–75]. Al_2O_3 was modified by MgO [78], MnO_x [79,80], FeO_x [79], CoO_x [79], NiO_x [79], ZnO_x [79,81], ZrO_x [81], BaO [82], and CeO_2 [83,84], and then loaded with gold for CO oxidation [78–80,82,84], CH_4 oxidation [81], and organic combustion [83]. On the other hand, because Au/TiO_2 is already quite active in CO oxidation, the further modification of the TiO_2 support was often overlooked [4]. For example, TiO_2 was modified by Al_2O_3 [22], MnO_2 [85], Fe_2O_3 [86,87], and ZnO [64], and then loaded with gold for CO oxidation [22,64,85,86] and methanol oxidation [87].

The complexity in assessing the previous literature lies in the fact that many of the reports mentioned above focused on the effect of additives on catalytic performance, but the gold catalysts were not often systematically treated at high temperatures to see whether they remained active or not. In addition, the fact that an additive was tried does not imply that it showed positive effect. Nevertheless, based on the limited and sometime contradictory results in the literature, it could be generalized that: (1) TiO_2/SiO_2 [29,30,54], MgO/Al_2O_3 [78], BaO/Al_2O_3 [82], and Al_2O_3/TiO_2 [22] could both stabilize gold particles and promote CO oxidation; (2) ZnO/Al_2O_3 [81] and ZrO_x/Al_2O_3 [81] could stabilize gold particles, but could not promote CH_4 oxidation; and (3) MnO_x/Al_2O_3 may or may not stabilize gold particles, but the MnO_x component could promote CO oxidation and CH_4 oxidation mainly as a co-catalyst or electronic promoter [78–81].

In fact, the stabilization of gold particles on supports is not limited to certain surface-modified oxides, but is also seen on certain mixed oxides or solid solutions. For instance, Goodman and coworkers found the stabilizing effect of the defect sites of TiO_2–SiO_2 by comparing the evolution of gold particles on TiO_2–SiO_2 and SiO_2 surfaces under vacuum [88]. Mou et al. [89] and Wan et al. [90] reported that Al^{3+} in Al-SBA-15 [89] or zeolite Y [90] could stabilize gold particles. Zheng and coworkers found that Fe_2O_3–ZrO_2 could stabilize gold particles, albeit Fe_2O_3–MnO_x, Fe_2O_3–CeO_2, Fe_2O_3–Co_2O_3, and Fe_2O_3–MoO_3 accelerated the sintering of gold [91].

A more thorough literature survey indicated that the stabilizing effect could go beyond the supported gold system. A 1990 review introduced that La_2O_3/Al_2O_3 could stabilize metallic nickel particles for CO methanation [33]. A similar effect was recently reported with $Cu/FeO_x/SiO_2$ [92], Cu–$B/Cr_2O_3/Al_2O_3$ [93], $Ni/ZrO_2/Al_2O_3$ [94], $Ni/La_2O_3/Al_2O_3$ [95], $Ni/CeO_2/Al_2O_3$ [95], and $Pt/CeO_2/ZrO_2$ [96] for various reactions. Recall that in the traditional synthesis of ammonia, Al_2O_3, CaO, and MgO promoters were used to minimize the sintering of metallic iron catalysts [1,2].

Thus, from the above literature survey, it could be argued that the effect of Al_2O_3 modification on stabilizing gold particles [22,28] is in fact not alone, and our current work involving 25 different surface additives apparently detected many modified gold catalysts not previously reported. Among the catalysts we surveyed, $Au/M_xO_y/TiO_2$ (M = Al, Ca, Ni, Zn, Ga, Y, Zr, La, Pr, Nd, Sm, Eu, Gd, Dy, Ho, Er, or Yb) exhibited small gold particle sizes even after 500 °C-aging, consistent with their high activities after 500 °C-aging. It is generally recognized that small gold particles are necessary for achieving high activity in CO oxidation, although gold particle size is not the only factor that determines the activity [3–9]. Our data are different from those of Scurrell et al. [64], who found that $Au/ZnO/TiO_2$ was less active than Au/TiO_2 in CO oxidation, probably due to different experimental conditions. Nevertheless, our data on $Au/ZnO/TiO_2$ and $Au/ZrO_2/TiO_2$ are in line with others' finding that ZnO/Al_2O_3 and ZrO_x/Al_2O_3 stabilized gold particles [81], although the supports and studied reactions are different. Our data are also in line with the finding that ZrO_2/Al_2O_3 [94] and La_2O_3/Al_2O_3 [33,95] stabilized nickel particles, although the underlying substrates, active metal, and catalyzed reactions are all different.

The question arises as to how certain additives or mixed oxides could stabilize metal particles. In principle, small metal particles possess extra surface free energy and higher chemical potential than those of the bulk metal [5,97]. Thus, metal atoms can move around even below the melting point of bulk metal, causing sintering [5,97]. Certain modified or mixed metal oxides may have surface defects [22,88–90] and so-called "spacers" [95] to hinder the movement of metal particles. A recent first-principle calculation proposed another model for $Au/IrO_2/TiO_2$, in which IrO_2 islands sit on top of TiO_2 surface, and Au particles sit on top of IrO_2 islands [98], so the migration of gold to an adjacent gold particle on another IrO_2 island is hindered by the large energy barrier across the TiO_2 surface [99]. Note that the stabilizing effect appears to be dependant on the nature of the combination of additive and support. For instance, although Al_2O_3 additive on TiO_2 [22] and Al^{3+} in Al_2O_3–SiO_2 mixed oxide [89,90] could stabilize gold particles, no significant promotional effect was seen on Al_2O_3 coatings dispersed on SiO_2 [23,26,72] or Al_2O_3–CeO_2 mixed oxide [100]. In addition, not all the additives are beneficial, as seen here with MoO_3, WO_3, SiO_2–WO_3, P_2O_5–WO_3, and Bi_2O_3 additives. Moreau and Bond also mentioned briefly that the addition of MoO_x to Au/TiO_2 significantly decreased the activity [62]. Further studies of the "support effects" [3,43,49,50] using surface science [88] and first-principle [99] methods should shed new light in these controversies.

In closing, the finding that a certain surface modifier such as Al_2O_3 on TiO_2 [22,28] could stabilize gold catalysts against

sintering actually points to a general methodology of using textural promoters in making metal catalysts [1,2]. Additional effects may include the change in electronic structure of the active metal and the supply of reactive oxygen caused by certain additives. Further research can be carried out based on the new catalyst system developed here. In particular, the nature of the active sites of gold catalysts has been highly debated [3–9], but virtually none of the catalysts used in these fundamental studies could achieve superior activity at −100°C. Thus, our newly developed highly active gold catalysts could be used as model catalysts in subsequent model studies on the nature of the active sites. In addition, considering the high activity of some promoted catalysts in CO oxidation, the selective CO oxidation in the presence of H_2 for fuel cell purposes could be possible and worth further research. From a historical perspective of the popularization of metal oxide-promoted mesoporous SiO_2 [69], SO_4^{2-}/ZrO_2 [70] and TiO_2 photocatalysts [71], it is predicted that the use of modified supports for gold catalysis may represent a promising direction for further research and development. In addition, considering the emerging applications of supported copper [101,102] and silver [103,104] nanoparticles, it is expected that this doping methodology may be extended to these systems to address the common sintering problem.

5. Conclusions

Au/TiO_2 is perhaps the most studied catalyst in gold catalysis research, but few attempts have been made to use surface-modified TiO_2 as support [3–9]. We have recently shown that Al_2O_3/TiO_2 synthesized by a surface sol–gel method could stabilize gold particles and improve the anti-aging ability [22,28]. Based on this key finding, in the present work we first attempted to synthesize $Au/Al_2O_3/TiO_2$ alternatively, and then developed a number of metal oxide-modified Au/TiO_2 catalysts. It was found that:

(1) The surface-sol–gel method [22,28] is not necessary to prepare highly active surface-modified gold catalysts. $Au/Al_2O_3/TiO_2$ prepared by the decomposition of $Al(NO_3)_3$ on TiO_2 followed by loading gold could show comparable performance in CO oxidation.
(2) Monolayer Al_2O_3 [22] is preferable to realize high activity in CO oxidation, but not absolutely necessary. Gold deposited on Al_2O_3/TiO_2 supports prepared with a range of calcination temperatures and Al_2O_3 contents could show significant activity.
(3) Al_2O_3 additive is not unique. Au/TiO_2 promoted by CaO, NiO, ZnO, Ga_2O_3, Y_2O_3, ZrO_2, La_2O_3, Pr_2O_3, Nd_2O_3, Sm_2O_3, Eu_2O_3, Gd_2O_3, Dy_2O_3, Ho_2O_3, Er_2O_3, or Yb_2O_3 could show significant activity at ambient temperature after 500 °C-aging.
(4) The promoted gold catalysts can undergo deactivation on stream. Although the sintering-resistant properties of gold on oxide supports were considerably improved via surface modification, no improvement on the corresponding temporal stability on stream was observed. However, the deactivated catalyst could be regenerated through thermal treatment, and the catalyst stability could be improved in the presence of H_2.

Acknowledgements

This work was supported by the Office of Basic Energy Sciences, U.S. Department of Energy. The Oak Ridge National Laboratory is managed by UT-Battelle, LLC for the U.S. DOE under Contract DE-AC05-00OR22725. This research was supported in part by the appointment for Z. Ma to the ORNL Research Associates Program, administered jointly by ORNL and the Oak Ridge Associated Universities.

Appendix A. Supplementary data

Supplementary data associated with this article can be found, in the online version, at doi:10.1016/j.molcata.2007.04.007.

References

[1] C.N. Satterfield, Heterogeneous Catalysis in Industrial Practice, 2nd ed., Krieger Publishing, Malabar, 1996.
[2] Z. Ma, F. Zaera, in: R.B. King (Ed.), Encyclopedia of Inorganic Chemistry, 2nd ed., John Wiley & Sons, Chichester, 2005, p. 1768.
[3] M. Haruta, Cattech 6 (2002) 102.
[4] A.S.K. Hashmi, G.J. Hutchings, Angew. Chem. Int. Ed. 45 (2006) 7896.
[5] G.C. Bond, C. Louis, D.T. Thompson, Catalysis by Gold, Imperial College Press, London, 2006.
[6] G.C. Bond, D.T. Thompson, Gold Bull. 33 (2000) 41.
[7] M. Haruta, M. Daté, Appl. Catal. A 222 (2001) 427.
[8] T.V. Choudhary, D.W. Goodman, Top. Catal. 21 (2002) 25.
[9] H.H. Kung, M.C. Kung, C.K. Costello, J. Catal. 216 (2003) 425.
[10] S. Biella, G.L. Castiglioni, C. Fumagalli, L. Prati, M. Rossi, Catal. Today 72 (2002) 43.
[11] P. Claus, Appl. Catal. A 291 (2005) 222.
[12] M.D. Hughes, Y.-J. Xu, P. Jenkins, P. McMorn, P. Landon, D.I. Enache, A.F. Carley, G.A. Attard, G.J. Hutchings, F. King, E.H. Stitt, P. Johnston, K. Griffin, C.J. Kiely, Nature 437 (2005) 1132.
[13] A. Corma, P. Serna, Science 313 (2006) 332.
[14] D. Andreeva, Gold Bull. 35 (2002) 82.
[15] Q. Fu, H. Saltsburg, M. Flytzani-Stephanopoulos, Science 301 (2003) 935.
[16] N. Sakulchaicharoen, D.E. Resasco, Chem. Phys. Lett. 377 (2003) 377.
[17] M. Yamada, M. Kawana, M. Miyake, Appl. Catal. A 302 (2006) 201.
[18] G. Pattrick, E. van der Lingen, C.W. Corti, R.J. Holliday, D.T. Thompson, Top. Catal. 30/31 (2004) 273.
[19] W.F. Yan, S.M. Mahurin, S.H. Overbury, S. Dai, Top. Catal. 39 (2006) 199.
[20] W.F. Yan, B. Chen, S.M. Mahurin, S. Dai, S.H. Overbury, Chem. Commun. (2004) 1918.
[21] W.F. Yan, B. Chen, S.M. Mahurin, V. Schwartz, D.R. Mullins, A.R. Lupini, S.J. Pennycook, S. Dai, S.H. Overbury, J. Phys. Chem. B 109 (2005) 10676.
[22] W.F. Yan, S.M. Mahurin, Z.W. Pan, S.H. Overbury, S. Dai, J. Am. Chem. Soc. 127 (2005) 10480.
[23] W.F. Yan, S.M. Mahurin, B. Chen, S.H. Overbury, S. Dai, J. Phys. Chem. B 109 (2005) 15489.
[24] Z. Ma, S. Brown, S.H. Overbury, S. Dai, Appl. Catal. A, submitted for publication.
[25] H.G. Zhu, C.D. Liang, W.F. Yan, S.H. Overbury, S. Dai, J. Phys. Chem. B 110 (2006) 10842.
[26] H.G. Zhu, Z. Ma, J.C. Clark, Z.W. Pan, S.H. Overbury, S. Dai, Appl. Catal. A 326 (2007) 89–99.

[27] W.F. Yan, S. Brown, Z.W. Pan, S.M. Mahurin, S.H. Overbury, S. Dai, Angew. Chem. Int. Ed. 45 (2006) 3614.
[28] S. Dai, W.F. Yan, Surface-Stabilized Gold Nanocatalysts, US Patent Application Publication, 2006/0293175 A1, 2006.
[29] Y. Tai, J. Murakami, K. Tajiri, F. Ohashi, M. Daté, S. Tsubota, Appl. Catal. A 268 (2004) 183.
[30] A.M. Venezia, F.L. Liotta, G. Pantaleo, A. Beck, A. Horvath, O. Geszti, A. Kocsonya, L. Guczi, Appl. Catal. A 310 (2006) 114.
[31] S.-J. Lee, A. Gavriilidis, J. Catal. 206 (2002) 305.
[32] C.K. Costello, M.C. Kung, H.-S. Oh, Y. Wang, H.H. Kung, Appl. Catal. A 232 (2002) 159.
[33] Y.C. Xie, Y.Q. Tang, Adv. Catal. 37 (1990) 1.
[34] Z. Ma, W.M. Hua, Y. Tang, Z. Gao, J. Mol. Catal. A 159 (2000) 335.
[35] X.G. Zhao, J.L. Shi, B. Hu, L.X. Zhang, Z.L. Hua, Mater. Lett. 58 (2004) 2152.
[36] Z.Y. Sun, Z.M. Liu, B.X. Han, S.D. Miao, Z.J. Miao, G.M. An, J. Colloid Interf. Sci. 304 (2006) 323.
[37] H. Araki, A. Fukuoka, Y. Sakamoto, S. Inagaki, N. Sugimoto, Y. Fukushima, M. Ichikawa, J. Mol. Catal. A 199 (2003) 95.
[38] O.V. Mokhnachuk, S.O. Soloviev, A.Y. Kapran, Catal. Today 119 (2007) 145.
[39] X.-F. Xu, J.Y. Jeon, M.H. Choi, H.Y. Kim, W.C. Choi, Y.-K. Park, J. Mol. Catal. A 266 (2006) 131.
[40] S.Y. Lai, H.X. Zhang, C.F. Ng, Catal. Lett. 92 (2004) 107.
[41] K. Qian, W.X. Huang, Z.Q. Jiang, H.X. Sun, J. Catal. 248 (2007) 137.
[42] W.M. Hua, Y.D. Xia, Y.H. Yue, Z. Gao, J. Catal. 196 (2000) 104.
[43] M. Comotti, W.C. Li, B. Spliethoff, F. Schüth, J. Am. Chem. Soc. 128 (2006) 917.
[44] W.-C. Li, M. Comotti, A.H. Lu, F. Schüth, Chem. Commun. (2006) 1772.
[45] A. Knell, P. Barnickel, A. Baiker, A. Wokaun, J. Catal. 137 (1992) 306.
[46] B. Schumacher, V. Plzak, M. Kinne, R.J. Behm, Catal. Lett. 89 (2003) 109.
[47] P. Konova, A. Naydenov, C. Venkov, D. Mehandjiev, D. Andreeva, T. Tabakova, J. Mol. Catal. A 213 (2004) 235.
[48] P. Konova, A. Naydenov, T. Tabakova, D. Mehandjiev, Catal. Commun. 5 (2004) 537.
[49] M.M. Schubert, S. Hackenberg, A.C. van Veen, M. Muhler, V. Plzak, R.J. Behm, J. Catal. 197 (2001) 113.
[50] S. Arrii, F. Morfin, A.J. Renouprez, J.L. Rousset, J. Am. Chem. Soc. 126 (2004) 1199.
[51] S. Carrettin, P. Concepción, A. Corma, J.M.L. Nieto, V.F. Puntes, Angew. Chem. Int. Ed. 43 (2004) 2538.
[52] N.S. Patil, B.S. Uphade, P. Jana, S.K. Bhargava, V.R. Choudhary, Chem. Lett. 33 (2004) 400.
[53] U.R. Pillai, S. Deevi, Appl. Catal. A 299 (2006) 266.
[54] W.F. Yan, B. Chen, S.M. Mahurin, E.W. Hagaman, S. Dai, S.H. Overbury, J. Phys. Chem. B 108 (2004) 2793.
[55] W.F. Yan, V. Petkov, S.M. Mahurin, S.H. Overbury, S. Dai, Catal. Commun. 6 (2005) 404.
[56] B.L. Zhu, Q. Guo, X.L. Huang, S.R. Wang, S.M. Zhang, S.H. Wu, W.P. Huang, J. Mol. Catal. A 249 (2006) 211.
[57] G.Y. Wang, W.X. Zhang, H.L. Lian, Q.S. Liu, D.Z. Jiang, T.H. Wu, React. Kinet. Catal. Lett. 75 (2002) 343.
[58] G.Y. Wang, W.X. Zhang, H.L. Lian, D.Z. Jiang, T.H. Wu, Appl. Catal. A 239 (2003) 1.
[59] B.T. Qiao, Y.Q. Deng, Appl. Catal. B 66 (2006) 241.
[60] X.Y. Deng, Z. Ma, Y.H. Yue, Z. Gao, J. Catal. 204 (2001) 200.
[61] M.S. Spencer, M.V. Twigg, Annu. Rev. Mater. Res. 35 (2005) 427.
[62] F. Moreau, G.C. Bond, Catal. Today 114 (2006) 362.
[63] B. Schumacher, V. Plzak, J. Cai, R.J. Behm, Catal. Lett. 101 (2005) 215.
[64] K. Mallick, M.S. Scurrell, Appl. Catal. A 253 (2003) 527.
[65] F. Moreau, G.C. Bond, Appl. Catal. A 302 (2006) 110.
[66] X.-H. Zou, S.-X. Qi, Z.-H. Suo, L.-D. An, F. Li, Catal. Commun. 8 (2007) 784.
[67] M. Manzoli, A. Chiorino, F. Boccuzzi, Appl. Catal. B 52 (2004) 259.
[68] M. Azar, V. Caps, F. Morfin, J.L. Rousset, A. Piednoir, J.C. Bertolini, L. Piccolo, J. Catal. 239 (2006) 307.
[69] D. Trong On, D. Desplantier-Giscard, C. Danumah, S. Kaliaguine, Appl. Catal. A 253 (2003) 545.
[70] X.M. Song, A. Sayari, Catal. Rev. -Sci. Eng. 38 (1996) 329.
[71] M.A. Fox, M.T. Dulay, Chem. Rev. 93 (1993) 341.
[72] M.T. Bore, M.P. Mokhonoana, T.L. Ward, N.J. Coville, A.K. Datye, Micropor. Mesopor. Mater. 95 (2006) 118.
[73] T.A. Nijhuis, B.J. Huizinga, M. Makkee, J.A. Moulijn, Ind. Eng. Chem. Res. 38 (1999) 884.
[74] E.E. Stangland, K.B. Stavens, R.P. Andres, W.N. Delgass, J. Catal. 191 (2000) 332.
[75] C.X. Qi, T. Akita, M. Okumura, M. Haruta, Appl. Catal. A 218 (2001) 81.
[76] M.A.P. Dekkers, M.J. Lippits, B.E. Nieuwenhuys, Catal. Today 54 (1999) 381.
[77] X.Y. Xu, J.J. Li, Z.P. Hao, W. Zhao, C. Hu, Mater. Res. Bull. 41 (2006) 406.
[78] R.J.H. Grisel, B.E. Nieuwenhuys, J. Catal. 199 (2001) 48.
[79] R.J.H. Grisel, B.E. Neiuwenhuys, Catal. Today 64 (2001) 69.
[80] D.H. Wang, Z.P. Hao, D.Y. Cheng, X.C. Shi, C. Hu, J. Mol. Catal. A 200 (2003) 229.
[81] A.C. Gluhoi, B.E. Nieuwenhuys, Catal. Today 119 (2007) 305.
[82] A.C. Gluhoi, X. Tang, P. Marginean, B.E. Nieuwenhuys, Top. Catal. 39 (2006) 101.
[83] M.A. Centeno, M. Paulis, M. Montes, J.A. Odriozola, Appl. Catal. A 234 (2002) 65.
[84] M.A. Centeno, C. Portales, I. Carrizosa, J.A. Odriozola, Catal. Lett. 102 (2005) 289.
[85] L.-H. Chang, N. Sasirekha, Y.-W. Chen, Catal. Commun., doi:10.1016/j.catcom.2006.08.050, in press.
[86] M. Shou, H. Takekawa, D.-Y. Ju, T. Hagiwara, D.-L. Lu, K. Tanaka, Catal. Lett. 108 (2006) 119.
[87] F.-W. Chang, H.-Y. Yu, L.S. Roselin, H.-C. Yang, T.-C. Ou, Appl. Catal. A 302 (2006) 157.
[88] B.K. Min, W.T. Wallace, D.W. Goodman, J. Phys. Chem. B 108 (2004) 14609.
[89] C.-W. Chiang, A.Q. Wang, B.-Z. Wan, C.-Y. Mou, J. Phys. Chem. B 109 (2005) 18042.
[90] J.-H. Chen, J.-N. Lin, Y.-M. Kang, W.-Y. Yu, C.-N. Kuo, B.-Z. Wan, Appl. Catal. A 291 (2005) 162.
[91] J.M. Hua, Q. Zheng, Y.H. Zheng, K.M. Wei, X.Y. Lin, Catal. Lett. 102 (2005) 99.
[92] C.-S. Chen, W.-H. Cheng, S.-S. Lin, Appl. Catal. A 257 (2004) 97.
[93] P.J. Guo, L.F. Chen, S.R. Yan, W.L. Dai, M.H. Qiao, H.L. Xu, K.N. Fan, J. Mol. Catal. A 256 (2006) 164.
[94] J.G. Seo, M.H. Youn, I.K. Song, J. Mol. Catal. A 268 (2007) 9.
[95] S. Natesakhawat, R.B. Watson, X.Q. Wang, U.S. Ozkan, J. Catal. 234 (2005) 496.
[96] S.M. Stagg-Williams, F.B. Noronha, G. Fendley, D.E. Resasco, J. Catal. 194 (2000) 240.
[97] A.W. Adamson, A.P. Gast, Physical Chemistry of Surfaces, 6th ed., John Wiley & Sons, New York, 1997.
[98] T. Akita, M. Okumura, K. Tanaka, S. Tsubota, M. Haruta, J. Electron. Microsc. 52 (2003) 119.
[99] Z.-P. Liu, S.J. Jenkins, D.A. King, Phys. Rev. Lett. 93 (2004) 156102.
[100] L. Ilieva, G. Pantaleo, I. Ivanov, A.M. Venezia, D. Andreeva, Appl. Catal. B 65 (2006) 101.
[101] O.P.H. Vaughan, G. Kyriakou, N. Macleod, M. Tikhov, R.M. Lambert, J. Catal. 236 (2005) 401.
[102] C.-H. Tu, A.-Q. Wang, M.-Y. Zheng, X.-D. Wang, T. Zhang, Appl. Catal. A 297 (2006) 40.
[103] Y.Y. Chen, C.A. Wang, H.Y. Liu, J.S. Qiu, X.H. Bao, Chem. Commun. (2005) 5298.
[104] J. Shen, W. Shan, Y.H. Zhang, J.M. Du, H.L. Xu, K.N. Fan, W. Shen, Y. Tang, J. Catal. 237 (2006) 94.